Studies of electron collisions with polyatomic molecules using distributed-memory parallel computers

C. Winstead, P. G. Hipes, M. A. P. Lima, and V. McKoy

Citation: The Journal of Chemical Physics **94**, 5455 (1991); doi: 10.1063/1.460480
View online: http://dx.doi.org/10.1063/1.460480
View Table of Contents: http://scitation.aip.org/content/aip/journal/jcp/94/8?ver=pdfcov
Published by the AIP Publishing

Studies of electron collisions with polyatomic molecules using distributed-memory parallel computers

C. Winstead, P. G. Hipes, M. A. P. Lima,[a] and V. McKoy
A. A. Noyes Laboratory of Chemical Physics, California Institute of Technology, Pasadena, California 91125

(Received 13 November 1990; accepted 10 January 1991)

Elastic electron scattering cross sections from 5–30 eV are reported for the molecules C_2H_4, C_2H_6, C_3H_8, Si_2H_6, and GeH_4, obtained using an implementation of the Schwinger multichannel method for distributed-memory parallel computer architectures. These results, obtained within the static-exchange approximation, are in generally good agreement with the available experimental data. These calculations demonstrate the potential of highly parallel computation in the study of collisions between low-energy electrons and polyatomic gases. The computational methodology discussed is also directly applicable to the calculation of elastic cross sections at higher levels of approximation (target polarization) and of electronic excitation cross sections.

I. INTRODUCTION

Studies of low-energy electron-molecule collisions by *ab initio* methods, although of much fundamental and practical interest, have proven much more difficult, and proceeded more slowly, than corresponding studies of bound-state electronic structure. In recent years there has been considerable progress both in the application of existing methods (see, for example, Refs. 1–4) and in the development of promising new approaches;[5-8] nevertheless, *ab initio* studies of molecules other than diatomics and linear triatomics remain relatively scarce, and have mostly been confined to small hydrides such as water,[9] ammonia,[10] methane,[1,5,11,12] and silane[13] (see, however, Refs. 7, 14, and 15).

The demand for data on the collision cross sections of low-energy electrons and gaseous polyatomics has continued to grow, owing to the expanding use of cold plasmas in the processing and fabrication of materials.[16] In nonequilibrium plasmas, the molecular species remain at temperatures of a few hundred Kelvin, while the electrons are accelerated to energies on the order of tens of electron volts. Collisions between these "hot" electrons and molecules generate reactive species—radicals, ions, and atoms—which can initiate useful chemistry, including etching, polymerization, boriding, nitriding, etc. A wide variety of gases is employed in plasma processing applications, including hydrocarbons such as CH_4, C_2H_4, and C_3H_8; other hydrides, such as PH_3, AsH_3, SiH_4, and Si_2H_6; and various fluorinated and chlorinated hydrocarbons, e.g., CCl_4, CH_3F, and C_2F_4. Many of these molecules are difficult and hazardous to work with experimentally, and information on the cross sections for even the most important species remains limited. This is especially true of the momentum transfer and excitation cross sections that are important in plasma modeling.

Considering the size of the molecules and range of processes involved, it seems clear that, if *ab initio* theory is to contribute to the understanding of low-temperature plasmas, significant availability of computing power, and theoretical methods which can exploit that power, will be required. As a step toward addressing this need, we have recently described[17] an implementation of the Schwinger multichannel (SMC) procedure[18,19] for the JPL/Caltech Mark IIIfp hypercube, a distributed-memory concurrent computer. Here, we report some initial studies using that implementation which, we feel, illustrate the great promise of highly parallel computation in the field of electron-molecule collisions. We have chosen to examine elastic scattering of low-energy electrons by a number of small polyatomics relevant to cold plasma technology, specifically C_2H_4, C_2H_6, C_3H_8, Si_2H_6, and GeH_4. These calculations, carried out within the static-exchange approximation, cover the energy range 5–30 eV, over which we find reasonable agreement with experimental data where measurements are available. Together with previously reported[11,13] studies of CH_4 and SiH_4, the present work also forms the basis for a preliminary examination of systematics in the electron scattering cross sections of X_nH_{2n+2} systems (X = C, Si, Ge). We will discuss below the possible relation between the position and width of shape resonances present in the cross sections of these molecules and the X–H bond length.

The present work serves in addition as a necessary prelude to studies planned or under way that will incorporate polarization and electronic excitation, and thus provide insight into the vibrational-excitation and dissociation phenomena which are of great importance in initiating plasma chemistry yet very difficult to determine experimentally. Such studies are not qualitatively more demanding than the present one and will be quite feasible on the generation of parallel machines which is currently becoming available, notably the Intel iPSC/860 hypercube and its mesh-connected successors. Prospects are thus very good both for obtaining highly accurate elastic cross sections, which will assist in determining total excitation cross sections from measured total scattering data, and for directly calculating reasonably accurate excitation cross sections for vibrational and low-lying electronic channels.

[a] Permanent address: Instituto de Física Gleb Wataghin, Unicamp, Caixa Postal 6165, 13081 Campinas, São Paulo, Brazil.

 131.2 0021-9606/91/085455-07$03.00

The remainder of this paper is organized as follows. In Sec. II we review the SMC method, outline its implementation for highly parallel computers, and give details of the present calculations. Cross sections for the various molecules are presented in Sec. III, while Sec. IV contains a discussion of the results and concluding remarks.

II. THEORETICAL AND COMPUTATIONAL

A. Schwinger multichannel method

The SMC method for obtaining low-energy electron-molecule scattering cross sections has been described previously,[18,19] so we recall here only its key features. In the SMC approach, the $(N+1)$-electron wave functions $\Psi_m^{(-)}(\mathbf{k}_m)$ and $\Psi_n^{(+)}(\mathbf{k}_n)$ of the electron-molecule scattering system are expanded in a basis set, and the coefficients of that expansion determined variationally by requiring that the scattering amplitude $f(\mathbf{k}_m,\mathbf{k}_n)$ be stationary. This leads to the expression

$$f(\mathbf{k}_m,\mathbf{k}_n) = -\frac{1}{2\pi}\sum_{ij}\langle S_m(\mathbf{k}_m)|V|\chi_i\rangle \times(\mathbf{A}^{-1})_{ij}\langle\chi_j|V|S_n(\mathbf{k}_n)\rangle, \quad (1)$$

for the scattering amplitude, where $S_m(\mathbf{k}_m)$ is an $(N+1)$-electron interaction-free or zeroth-order function of the form

$$S_m(\mathbf{k}_m) = \Phi_{\text{target}}^{(m)}(1,2,...,N)\exp(i\mathbf{k}_m\cdot\mathbf{r}_{N+1}), \quad (2)$$

V is the interaction between the target and the scattered electron, and χ_i are elements of the expansion basis. The $(\mathbf{A}^{-1})_{ij}$ are elements of the inverse of the matrix $\langle\chi_i|A^{(+)}|\chi_j\rangle$, where $A^{(+)}$ is given by

$$A^{(+)} = \frac{1}{2}(PV+VP) - VG_P^{(+)}V - \frac{1}{N+1}\left\{\hat{H} - \frac{N+1}{2}(\hat{H}P+P\hat{H})\right\}. \quad (3)$$

In this expression, P is a projector onto open channels,

$$P = \sum_{l\in\text{open}}|\Phi_l(1,2,...,N)\rangle\langle\Phi_l(1,2,...,N)|, \quad (4)$$

and $G_P^{(+)}$ is the projected Green's function. In Eq. (3), $\hat{H} = (E-H)$, where E is the total energy of the system and H is the full Hamiltonian.

In our implementation, the basis χ_i consists of $(N+1)$-electron Slater determinants of molecular orbitals, which are in turn expanded in Cartesian Gaussian functions

$$N_{lmn}(x-A_x)^l(y-A_y)^m(z-A_z)^n\exp(-\alpha|\mathbf{r}-\mathbf{A}|^2), \quad (5)$$

widely used in bound-state quantum chemistry. With this choice, all matrix elements required in Eq. (1) for $f(\mathbf{k}_m,\mathbf{k}_n)$, except those involving $VG_P^{(+)}V$, can be computed analytically. The $VG_P^{(+)}V$ matrix elements are obtained by numerical quadrature over the momentum variable occurring in a spectral representation of the Green's function.[20]

B. Parallel implementation

The computationally intensive step in the SMC procedure as formulated above is the evaluation of the primitive two-electron integrals

$$\langle\alpha\beta|V|\gamma\mathbf{k}\rangle = \int\int d^3\mathbf{r}_1\, d^3\mathbf{r}_2\,\alpha(\mathbf{r}_1)\beta(\mathbf{r}_1)\times\frac{1}{r_{12}}\gamma(\mathbf{r}_2)e^{i\mathbf{k}\cdot\mathbf{r}_2}, \quad (6)$$

which involve three Cartesian Gaussians α, β, and γ, and a plane wave $e^{i\mathbf{k}\cdot\mathbf{r}}$. These integrals must be obtained for all distinct combinations of α, β, and γ, and for a wide range of k in both direction and magnitude. Although they are evaluated analytically, their computation nevertheless consumes the bulk of the computer time, simply because the number of such integrals required is so large.

The fact that most of the computation in the SMC procedure is concentrated in the evaluation of the primitive integrals makes it attractive to consider implementing the SMC method on a parallel computer architecture, permitting the calculation of various subsets of the primitive integrals to proceed concurrently. A parallel approach is especially appealing since the integral-evaluation algorithms involve recursive steps that inhibit vectorization on CRAY-type machines. As described in detail elsewhere,[17] we have found a parallel version of the SMC method quite successful as implemented for the Mark IIIfp hypercube computer.

The Mark IIIfp,[21] developed at the Jet Propulsion Laboratory, is a multiple-instruction, multiple-data (MIMD) machine of the distributed-memory type.[22] Its individual processing elements, or nodes, are fairly powerful microprocessor-based computers, incorporating accelerator boards for 64-bit floating-point arithmetic and substantial memory (4 megabytes/node). The nodes operate autonomously, communicating with each other and with the front end via message-passing routines over a communications net with hypercube topology. The Mark IIIfp design allows for up to 128 such nodes in a single machine, thus achieving aggregate processing speed and central memory comparable to those of conventional supercomputers.[23]

Because of the large memory per node, the entire primitive-integral package from the original SMC code can run intact on each processor, accumulating a subset of the required primitive integrals in the processor memory. Transformation from the primitive integrals to matrix elements needed in Eq. (1) is achieved in an efficient and regular fashion by exploiting distributed matrix-multiplication algorithms. A similar strategy is employed in certain integration steps that also require interprocessor communication. The solution of a system of linear equations occurring in the final stages of the calculation is also achieved on the hypercube using an adaptation of a distributed LU solver[24] for complex arithmetic.

In comparisons for elastic electron-CO scattering in a fairly small basis set, we have found that the performance of the hypercube SMC code surpasses that of the original code running on one CRAY Y-MP CPU for as few as 32 Mark IIIfp nodes, while performance on a 64-node Mark IIIfp, the largest currently available, is approximately a factor of 3 greater than on the CRAY.[17] Speedup factors for larger problems, such as those reported below, are likely to be still more favorable, since the ratio of computation to inter-

processor communication overhead is increased;[25] however, the CRAY execution times for these problems are not available for comparison.

C. COMPUTATIONAL DETAILS

All of the calculations reported below were carried out within the static-exchange approximation, and thus neglect polarization of the target by the scattering electron. Based on previous experience,[9-11,13] we do not expect this to be a serious limitation at energies above 5 eV, except in shifting the positions of resonance features toward higher energy by about 1–3 eV.

The contracted Gaussian basis sets used for both the electronic structure calculations on the target molecules and construction of the scattering basis were as follows. For C, we used the $(9s5p)/[4s3p]$ set of Dunning,[26] supplemented by one s, one p, and one d orbital, with exponents 0.0473, 0.0365, and 0.06, respectively. The Si basis used was the $(12s8p)/[4s2p]$ set of McClean and Chandler,[27] supplemented by two s orbitals (exponents 0.05 and 0.02), two p orbitals (exponents 1.0 and 0.05), and two d orbitals (exponents 0.2 and 0.07). For Ge we used the $(14s11p5d)$ basis of Huzinaga.[28] Two comparable $(4s)/[3s]$ basis sets were used for H; the Si_2H_6 and GeH_4 calculations used that of Pacansky and Dupuis,[29] while the remaining calculations employed that of Dunning.[26] All calculations were carried out at fixed nuclear geometries.[30-34]

No detailed study was made of the basis set dependence of the results; however, a larger basis set was tested for C_2H_6 and found to make little difference. Similar basis sets gave converged results in previous studies[13,20] on SiH_4 and CH_4, where it was also possible to compare to results obtained in larger bases. We therefore do not believe basis set limitations to be a major source of error in the present work. Convergence of the numerical quadrature for $VG_P^{(+)}V$ was tested in all cases, and it is believed that errors arising from this source amount to no more than a few percent over the range of energies studied. Further refinement does not appear warranted in light of the intrinsic limitations of the fixed-nuclei static-exchange model.

III. RESULTS

We have calculated differential elastic, integral elastic, and momentum-transfer cross sections at a number of energies for each of the molecules C_2H_4, C_2H_6, C_3H_8, GeH_4, and Si_2H_6. Tabulated values of these cross sections are available on request. Below we present representative results, emphasizing cases where experimental data is available for comparison. Since the static-exchange level of theory is not sufficient to give highly quantitative predictions, we compare our integrated elastic results both with elastic and with total experimental cross sections, with the aim of giving some measure of the general quality of the calculations. This seems appropriate since the experimental integrated elastic results, where available at all, may be subject to large uncertainties.

Integral elastic cross sections for C_2H_4, C_2H_6, and C_3H_8 are shown in Fig. 1, which also includes the CH_4 cross section[11] for purposes of comparison. Selected experimental data shown include integrated elastic differential cross sections[35,36] for CH_4 and C_2H_6 as well as total cross sections obtained by transmission measurements[37-39] for each molecule. The latter include contributions from electronically inelastic scattering at higher energies. These contributions appear to be quite large above 15 eV. To our knowledge no theoretical cross sections have yet been published for C_2H_4, C_2H_6, or C_3H_8. Other static-exchange calculations for e^-—CH_4 scattering[5,12] generally agree well with the curve shown in Fig. 1.

The present calculations appear to give fairly reliable results for the integral elastic cross sections. Specifically, our

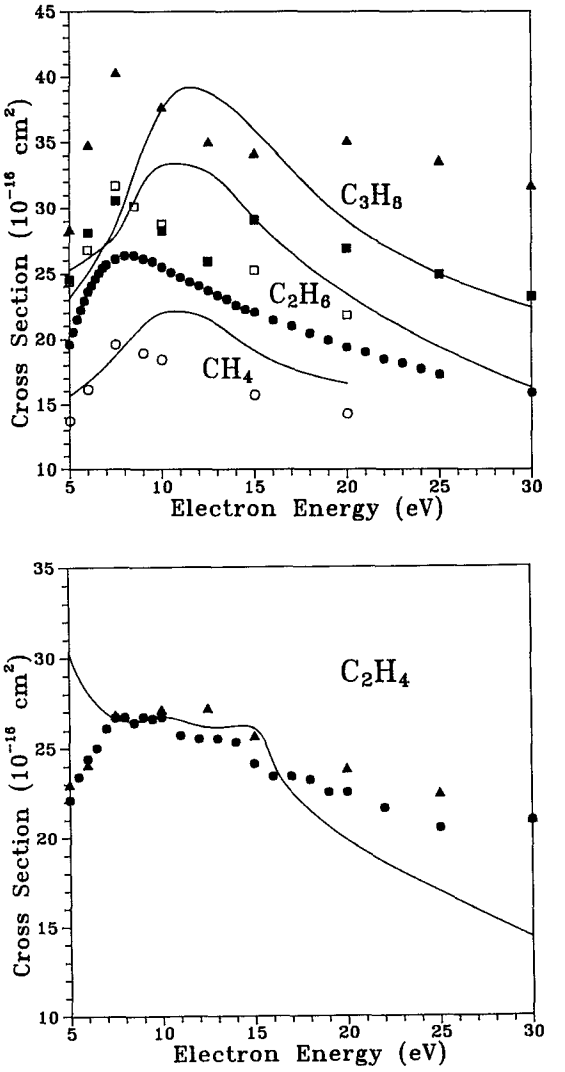

FIG. 1. (a) Integral elastic cross sections for electron scattering by CH_4, C_2H_6, and C_3H_8. Solid curves are static-exchange results (CH_4 results from Ref. 11). Experimental points shown are total cross sections for CH_4 (filled circles), C_2H_6 (filled squares) and C_3H_8 (solid triangles) from Refs. 37 (CH_4) and 39; and integrated differential elastic cross sections for CH_4 (open circles) and C_2H_6 (open squares) from Refs. 35 and 36, respectively. (b) Integral elastic cross section for C_2H_4 in the static-exchange approximation (solid curve). Experimental points are total cross section measurements of Ref. 38 (circles) and 39 (triangles).

results have the correct overall magnitudes, and for C_2H_6 and C_3H_8 reproduce the well-known[40] broad shape resonance. However, the position of the resonance maximum is shifted to higher energy in the static-exchange approximation: whereas the experimental maxima are located at roughly 7.5 eV, as in CH_4, the maxima in the calculated curves fall at approximately 10 eV. These shifts are comparable to that seen in CH_4 (Fig. 1) and indeed are to be expected when polarization of the target is neglected.

The C_2H_4 cross section is somewhat more complicated. Although not shown on the figure, the experimentally observed low-energy (2 eV) shape resonance[38] in C_2H_4 is present in the static-exchange cross section, but shifted toward higher energy. The tail of this resonance extends above 5 eV, enhancing the calculated cross section at the lowest energies shown in Fig. 1. At higher energies, the calculated cross section shows indications of overlapping resonances at about 10 and 14 eV. This energy region will be discussed further below.

In Fig. 2 the integral elastic cross sections for Si_2H_6 and GeH_4 are shown. For comparison, the cross section for SiH_4 obtained in an earlier study[13] is also given. Experimental total cross section[41] and integrated elastic[42] data for SiH_4 are plotted; we are not aware of any such data for Si_2H_6 or GeH_4, although differential scattering cross-section measurements have been reported[43] for Si_2H_6 (see below). Examining Fig. 2, we see that the Si_2H_6 cross section is approximately a factor of 1.5 larger than that for SiH_4. A similar ratio is observable in Fig. 1 between the C_2H_6 and CH_4 cross sections. Likewise, a shape resonance is seen in Si_2H_6 below 5 eV, near the energy where one is observed in SiH_4, as was the case in the alkane series. However, the cross sections for the silicon-containing molecules are much larger than those for the corresponding hydrocarbons shown in Fig. 1, and the resonances lie at much lower energies. The larger cross sections of the Si species are attributable in most part simply to their greater geometric size. Consistent with this explanation is the similarity in magnitude of the GeH_4 and SiH_4 cross sections, the Ge–H bond length in GeH_4, 1.527 Å, being quite close to the Si–H bond length in SiH_4, 1.480 Å. There also appears to be a connection between the X–H (X = C, Si, Ge) bond length and the resonance position, which will be discussed in detail in the next section.

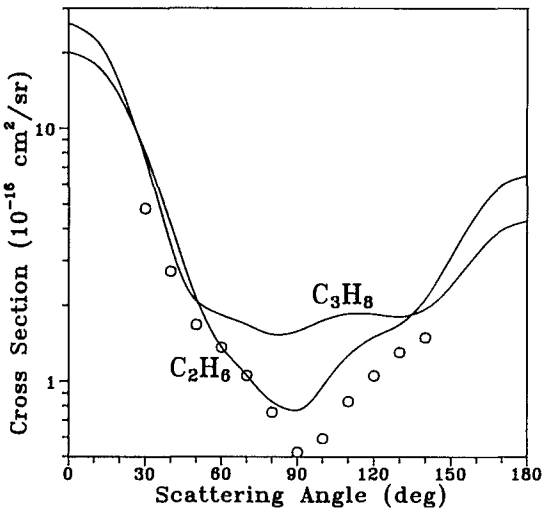

FIG. 3. Differential elastic cross sections for C_2H_6 and C_3H_8 at 10 eV, including measurements of Ref. 36 for C_2H_6 (circles).

Differential cross sections for C_2H_4, C_2H_6, C_3H_8, Si_2H_6, and GeH_4 are shown at selected energies in Figs. 3–6. Experimental data[36,43] are included in the figures where available. In general, there is good agreement between our results and these measured values.

In Figs. 7 and 8 we present the momentum-transfer

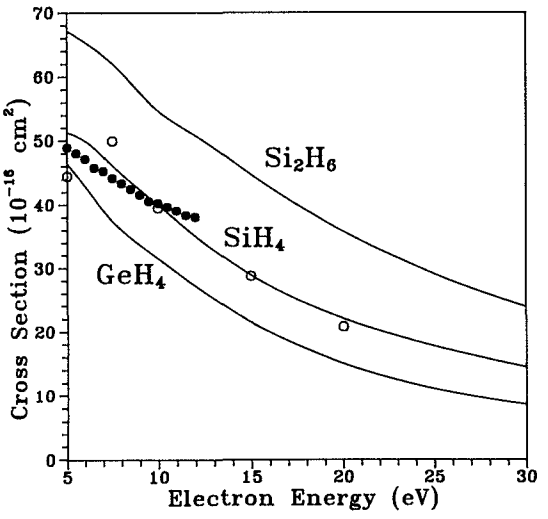

FIG. 2. Integral elastic cross sections in the static-exchange approximation for SiH_4 (Ref. 13), GeH_4, and Si_2H_6. Experimental points for SiH_4 are total cross section measurements (solid circles) of Ref. 41 and angle-integrated elastic values of Ref. 42 (open circles).

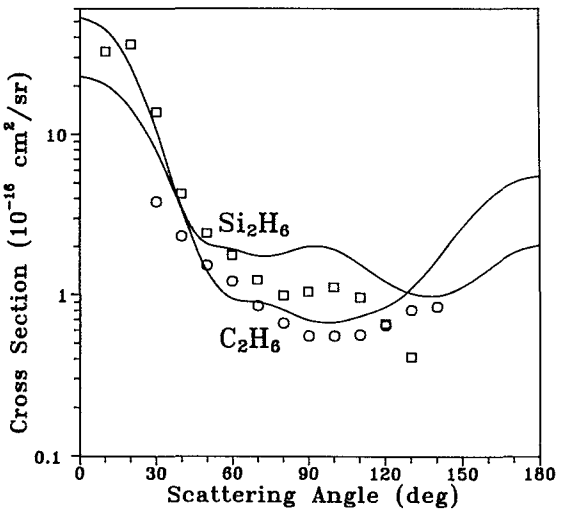

FIG. 4. Differential elastic cross sections for C_2H_6 and Si_2H_6 at 15 eV, including measurements of Ref. 36 for C_2H_6 (circles) and Ref. 43 for Si_2H_6 (squares).

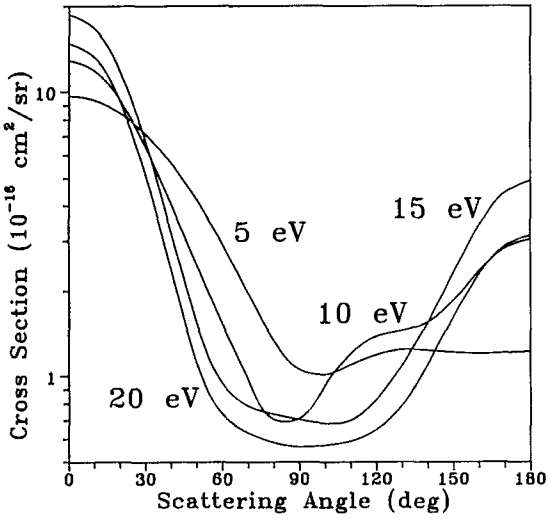

FIG. 5. Differential elastic cross section for C_2H_4 at 5, 10, 15, and 20 eV.

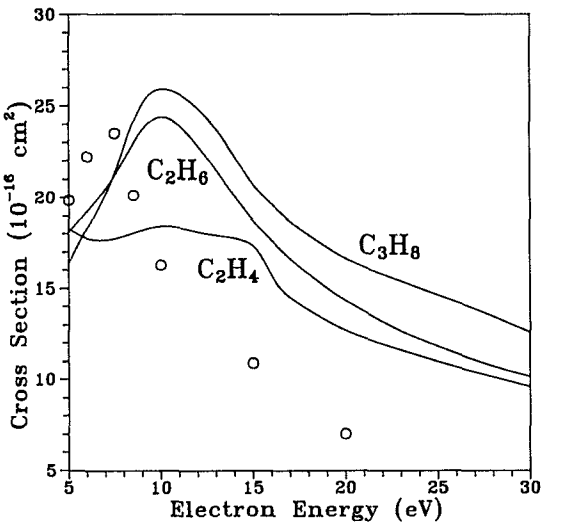

FIG. 7. Momentum-transfer cross sections for C_2H_4, C_2H_6, and C_3H_8. Open circles are values of Ref. 36 for C_2H_6, derived from the measured differential cross section.

cross sections for the five molecules we have studied, along with experimental values for C_2H_6.[36] Results for silane[13,42] are included in Fig. 8 for comparison. The momentum-transfer cross sections follow the trend of the integral cross section fairly closely, as may be seen in comparing Figs. 7 and 8 to Figs. 1 and 2. There is a large discrepancy between the experimental and theoretical momentum-transfer cross sections for C_2H_6 that is only partially accounted for by the shift in the resonance position. Our differential cross section for C_2H_6 nevertheless agrees fairly well with the experimental data over the range where measurements were made (see Figs. 3 and 4). However, we find the scattering at smaller and larger angles to be unusually large, and the disagreement in the momentum-transfer cross sections may thus be due to the extrapolation of the measured differential cross section at large angles. Agreement with the integral cross section derived from the same data is much better (Fig. 1), since the large-angle scattering is not as heavily weighted in this case.

IV. DISCUSSION

The present study has several goals: first, to provide reasonably accurate theoretical elastic cross sections for some molecules currently of interest in low-temperature plasma applications; second, to explore some trends in the cross sections of these molecules; third, to test the reliability of the static-exchange approximation for somewhat larger systems than it has usually been applied to in the past; and fourth, to demonstrate the potential of highly parallel computers in electron-scattering applications.

Regarding the first and third objectives, the reliability of

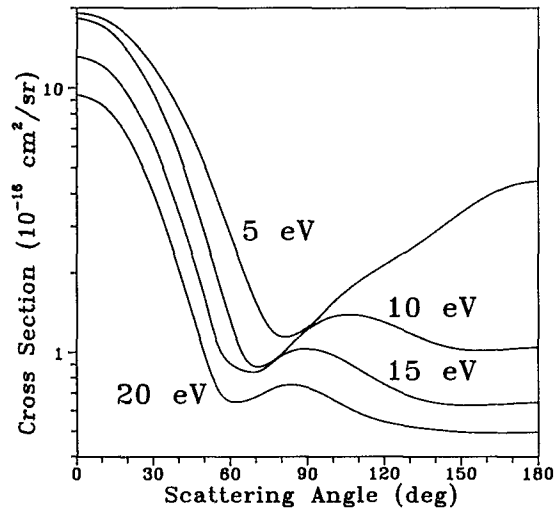

FIG. 6. Differential elastic cross section for GeH_4 at 5, 10, 15, and 20 eV.

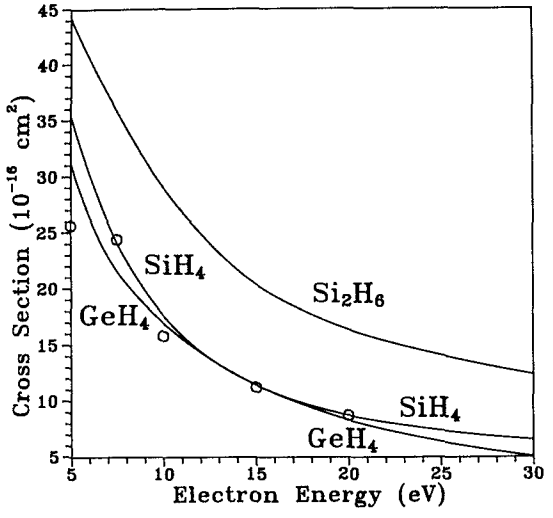

FIG. 8. Momentum-transfer cross sections for SiH_4 (Ref. 13), GeH_4, and Si_2H_6. Open circles are values of Ref. 42 for SiH_4, derived from the measured differential cross section.

the present static-exchange results may be gauged from the agreement with experiment in those cases where measurements have been reported. Such a comparison indicates that, as for smaller systems,[9-11,13] the static-exchange approximation is sufficient to yield the correct overall magnitude of the integral and momentum-transfer cross sections, and the correct general shape of the differential cross section. The static-exchange approximation does not position resonances correctly, nor does it give differential cross sections that are correct in detail, especially at lower energies. However, since resonances are systematically shifted, always appearing at too high an energy, static-exchange calculations can form the basis for an accurate estimate of the true cross section. This is an important consideration, since more elaborate calculations may not be feasible for still larger molecules than those considered here.

We have observed two principal trends in the molecules we have studied. One is a fairly straightforward and unsurprising dependence of the integral cross section on molecular size. More interesting is the relation between resonance positions in these X_nH_{2n+2} compounds and X–H bond length. All of the carbon compounds studied have similar C–H bond lengths (respectively, 1.09, 1.07, 1.11, and 1.09 Å in CH_4, C_2H_4, C_2H_6, and C_3H_8), and each exhibits a broad shape resonance maximum at about 7.5 eV. The Si–H and Ge–H bond distances are considerably longer than the C–H distances (1.48, 1.53, and 1.53 Å, respectively, in SiH_4, Si_2H_6, and GeH_4), and the shape resonance in each of these molecules occurs significantly lower in energy than in its carbon analog.

In the XH_4 molecules, there is a direct relation between the X–H bond length and the size of the molecule. A simple particle-in-box model of the resonance would therefore suffice to predict that longer bond length would correlate with lower resonance energy. However, the "size" of a molecule such as propane is determined more by the length of the carbon chain than by that of the C–H bond. Nevertheless, the broad maximum in propane (and even butane[39,40]) occurs at the same energy as that in methane. Likewise, the SiH_4 and Si_2H_6 resonance maxima occur at nearly the same energy. Thus the resonance seems to be associated with the X–H bond itself, presumably as temporary trapping in an antibonding X–H orbital. Indeed, there is evidence from experimental studies of vibrational excitation to support this view.[44,45]

Arguing against the above interpretation is the well-known analogy between the CH_4 and SiH_4 resonances and the d-wave shape resonances observed in argon, krypton, and xenon, which are explainable in terms of the $l = 2$ angular-momentum barrier. That similar resonances occur in these noble gases certainly suggests that the X–H antibonding orbitals are not the whole story. The differential cross sections of both CH_4 and SiH_4 do in fact reflect substantial d-wave character in the resonance region.[35,42] However, in T_d symmetry the $l = 2$ partial wave transforms according to both the T_2 and the E representations, yet the resonance in CH_4 and SiH_4 occurs only in T_2, which is the symmetry of the unoccupied antibonding valence orbital. There need not be a total dichotomy between the angular momentum barrier and valence orbital interpretations; both may contribute to formation of the resonance. The location of the resonance appears, however, to correlate better with the location of the appropriate virtual orbital than with the most pronounced d-wave character in the differential cross section. Experimentally, the d-wave pattern is most evident at about 3–4 eV in both methane[35] and silane,[42] for instance, while the resonance maximum lies in this range only for silane.

In a molecule such as propane one might expect to find several shape resonances, since there are inequivalent hydrogen atoms and more than one virtual valence orbital has C–H antibonding character. We do not see any clear evidence of this in our results, possibly because the resonances are so broad as to merge together. On the other hand, we do see a suggestion of a multiple resonance structure in C_2H_4, with maxima at 10 and 14 eV. Vibrational-excitation measurements have also indicated that two resonances may be present.[44] More elaborate studies of this molecule, including vibrational excitation cross sections, are currently under way in our group.

The results we have presented here demonstrate the potential of highly parallel supercomputers in the field of electron-molecule scattering. We found that the conversion of our existing sequential program to a distributed-memory concurrent implementation, while not straightforward, was accomplished in a reasonable amount of time, and that the performance of the resulting code on the Mark IIIfp amply rewarded this effort. While we are continuing to make improvements to the program, the greatest performance increase in the future is likely to be due to improved hardware. The newest commercial distributed-memory machines, notably the Intel iPSC/860, promise per-node performance far above that of the Mark IIIfp, as well as larger memory per node and, significantly, more than 128 nodes. Both the absolute performance and the price/performance ratio of such machines will make them highly attractive for computationally intensive work, provided that the methods employed in that work are suitable for a parallel implementation.

ACKNOWLEDGMENTS

It is a pleasure to thank the following individuals for their encouragement and support of this work: Don Austin of the Department of Energy; Terry Cole, Dave Curkendall, and Edith Huang of JPL; and Geoffrey Fox, Paul Messina, and Heidi Lorenz-Wirzba of the Caltech Concurrent Computation Program. Parallel computing facilities were provided by the Hypercube Project of JPL and the Caltech Concurrent Supercomputing Facility. Support by the Applied Mathematical Sciences Program of the Department of Energy, the Strategic Defense Initiative Organization through the Army Research Office, the National Science Foundation (PHY-8901515 and INT-8714948), and JPL is also gratefully acknowledged.

Work at the California Institute of Technology was supported by the Air Force Office of Scientific Research through Grant No. AFOSR-89-0132. Portions of these calculations made use of resources provided by the JPL/Caltech Supercomputing Project and by the National Center for

Supercomputing Applications at the University of Illinois, which is supported by the National Science Foundation.

[1] M. A. P. Lima, K. Watari, and V. McKoy, Phys. Rev. A **39**, 4312 (1989).
[2] H. P. Pritchard, V. McKoy, and M. A. P. Lima, Phys. Rev. A **41**, 546 (1990).
[3] S. E. Branchett and J. Tennyson, Phys. Rev. Lett. **64**, 2889 (1990).
[4] C. J. Gillan, C. J. Noble, and P. G. Burke, J. Phys. B **23**, L407 (1990).
[5] P. McNaughten and D. G. Thompson, J. Phys. B **21**, L703 (1988).
[6] T. N. Rescigno and B. I. Schneider, J. Phys. B **21**, L691 (1988).
[7] T. N. Rescigno, C. W. McCurdy, and B. I. Schneider, Phys. Rev. Lett. **63**, 248 (1989).
[8] T. N. Rescigno, B. H. Lengsfield, and C. W. McCurdy, Phys. Rev. A **41**, 2462 (1990).
[9] L. M. Brescansin, M. A. P. Lima, T. L. Gibson, and V. McKoy, J. Chem. Phys. **85**, 1854 (1986).
[10] H. P. Pritchard, M. A. P. Lima, and V. McKoy, Phys. Rev. A **39**, 2392 (1989).
[11] M. A. P. Lima, T. L. Gibson, and V. McKoy, Phys. Rev. A **32**, 2696 (1985).
[12] C. W. McCurdy and T. N. Rescigno, Phys. Rev. A **39**, 4487 (1989).
[13] C. Winstead and V. McKoy, Phys. Rev. A **42**, 5357 (1990).
[14] W. M. Huo, Phys. Rev. A **38**, 3303 (1988).
[15] B. I. Schneider, T. N. Rescigno, and C. W. McCurdy, Phys. Rev. A **42**, 3132 (1990).
[16] *Plasma Reactions and Their Applications*, Japan Materials Report by Japan Technical Information Service (ASM International, Metals Park, OH, 1988).
[17] P. Hipes, C. Winstead, M. Lima, and V. McKoy, *Proceedings of the Fifth Distributed Memory Computing Conference, Vol. I: Applications*, edited by D. W. Walker and Q. F. Stout (IEEE Computer Society, Los Alamitos, CA, 1990), p. 498.
[18] K. Takatsuka and V. McKoy, Phys. Rev. A **24**, 2473 (1981).
[19] K. Takatsuka and V. McKoy, Phys. Rev. A **30**, 1734 (1984).
[20] M. A. P. Lima, L. M. Brescansin, A. J. R. da Silva, C. Winstead, and V. McKoy, Phys. Rev. A **41**, 327 (1990).
[21] E. Huang, E. Jennings, R. Lee, J. Patterson, A. Sides, J. St. Henri, and E. Upchurch, *Mark III User's Introductory Guide*, Report D-5304 (Jet Propulsion Laboratory, 1989); *Hypercube Project Programmer's Manual, Rev. D*, Report D-3220 (Jet Propulsion Laboratory, 1989).
[22] G. Fox, M. Johnson, G. Lyzenga, S. Otto, J. Salmon, and D. Walker, *Solving Problems on Concurrent Processors* (Prentice-Hall, Englewood Cliffs, NJ, 1988), Vol. I, p. 22.
[23] H.-Q. Ding and M. S. Makivić, Phys. Rev. Lett. **64**, 1449 (1990).
[24] P. G. Hipes, Caltech Concurrent Computation Program Report C^3P-652b (1989).
[25] Reference 22, p. 50 ff.
[26] T. H. Dunning, J. Chem. Phys. **53**, 2823 (1970).
[27] A. D. McClean and G. S. Chandler, J. Chem. Phys. **72**, 5639 (1980).
[28] S. Huzinaga, J. Chem. Phys. **66**, 4245 (1977).
[29] J. Pacansky and M. Dupuis, J. Chem. Phys. **68**, 4277 (1978).
[30] J. M. Schulman, J. W. Moskowitz, and C. Hollister, J. Chem. Phys. **46**, 2759 (1967).
[31] A. Almenningen and O. Bastiansen, Acta Chem. Scand. **9**, 815 (1955).
[32] D. R. Lide, Jr., J. Chem. Phys. **33**, 1514 (1960).
[33] B. Beagley, A. R. Conrad, J. M. Freeman, J. J. Monaghan, and B. G. Norton, J. Mol. Struct. **11**, 371 (1972).
[34] L. P. Lindeman and M. K. Wilson, J. Chem. Phys. **22**, 1723 (1954).
[35] H. Tanaka, T. Okada, L. Boesten, T. Suzuki, T. Yamamoto, and M. Kubo, J. Phys. B **15**, 3305 (1982).
[36] H. Tanaka, L. Boesten, D. Matsunaga, and T. Kudo, J. Phys. B **21**, 1255 (1988).
[37] R. K. Jones, Phys. Rev. A **82**, 5424 (1985).
[38] O. Sueoka and S. Mori, J. Phys. B **19**, 4035 (1986).
[39] K. Floeder, D. Fromme, W. Raith, A. Schwab, and G. Sinapius, J. Phys. B **18**, 3347 (1985), and private communication.
[40] E. Brüche, Ann. Phys. (Leipzig) **4**, 387 (1930).
[41] H.-X. Wan, J. H. Moore, and J. A. Tossell, J. Chem. Phys. **91**, 7340 (1989).
[42] H. Tanaka, L. Boesten, H. Sato, M. Kimura, M. A. Dillon, and D. Spence, J. Phys. B **23**, 577 (1990).
[43] H. Tanaka, L. Boesten, H. Sato, M. Kimura, M. A. Dillon, and D. Spence, 42nd Annual Gaseous Electronics Conference, Palo Alto, 1989, and private communication.
[44] I. C. Walker, A. Stamatovic, and S. F. Wong, J. Chem. Phys. **69**, 5532 (1978).
[45] F. Motte-Tollet, M.-J. Hubin-Franskin, and J. E. Collin, J. Chem. Phys. **93**, 7843 (1990), and private communication.